Multisource excitations in a stratified biphase structure

Wenwu Cao[a] and Wenkang Qi
Materials Research Laboratory, The Pennsylvania State University, University Park, Pennsylvania 16802

(Received 6 March 1995; accepted for publication 22 June 1995)

A stratified biphase structure can have many mechanical resonance modes due to the existence of several length scales in the system. The resonance effect is greatly enhanced if there are periodic synchronized multiple driving sources in the structure. For example, a single beam or a linear array composite transducers used in medical ultrasonic imaging. Such resonance behavior can be studied using an extended transfer matrix technique which we name: multisource T-matrix technique. Using this technique we have studied the effects of randomization in a 2-2 composite. It is found that for dispersing the pitch resonance the randomization of ceramic spacing is more effective for low ceramic content, while randomization of ceramic width is more effective for high ceramic content. © *1995 American Institute of Physics.*

I. INTRODUCTION

Transfer matrix (T matrix) is one of the tools used in the study of wave propagation characteristics in stratified structures.[1–9] In all the previous studies using T matrix, the Floquet relation must be used to derive the dispersion relation. However, the Floquet relation is valid only for an infinite system, it is not appropriate to use it for a finite system. On the other hand, the transfer matrix technique can be used for systems of any size so long as the wave propagation has one-dimensional nature. With this consideration recently we have introduced a definition of a complex wave number $\tilde{k}$ using the T matrix alone so that the dispersion relation can be derived for a finite system without the Floquet condition.[10] Using this new definition the development of band structures with the increase of the number of cells in the composite can be calculated directly.

In a 2-2 composite transducer, the active components are often driven simultaneously. In other words, there are more than one wave sources in the structure. For such systems, the band structure study, which only deals with single-wave propagation, would not be as useful since new resonance feature will be produced by the interference of multiwave sources. There will be interference between the incident and reflected waves, and also among waves of different sources.

Although of practical importance, theoretical studies on such multisource driven system have not been reported in the literature. It is the intention of this paper to extend the transfer matrix technique to address this problem.

A typical single beam 2-2 composite transducer is shown in Fig. 1, where the piezoelectric ceramics are the active components of the transducer and the polymers are the passive components. When an electric potential is applied to the transducer through the top and bottom electrodes, the ceramic components will either contract or expand to generate acoustic signals through piezoelectric coupling, whereas the polymer components will play the passive role of damping and acoustic coupling agent to a low acoustic impedance medium.

In reality, the resonance behavior of the system shown in Fig. 1 depends on both the position of the driving source and the number of the driving sources. For simplicity, we assume the system to be linear, so that the principle of superposition can be used.

Following the spirit of the single-source transfer matrix technique, we introduce here an algorithm of multisource transfer matrix for the study of stratified structures. Quantitative calculations have been carried out for a 2-2 ceramic-polymer composite as shown in Fig. 1 with both periodic and random arrangements. We choose the shear wave as an example for this study, other waves can be studied in a similar fashion.

II. TRANSFER MATRIX FOR MULTISOURCE DRIVEN 2-2 COMPOSITES

As shown in Fig. 1, when all the ceramic elements are being driven in the z direction with an alternating field, shear waves are being generated at all the ceramic-polymer interfaces. It can be shown (Appendix) that for a linear system the wave functions in the nth cell can be written in the following from:

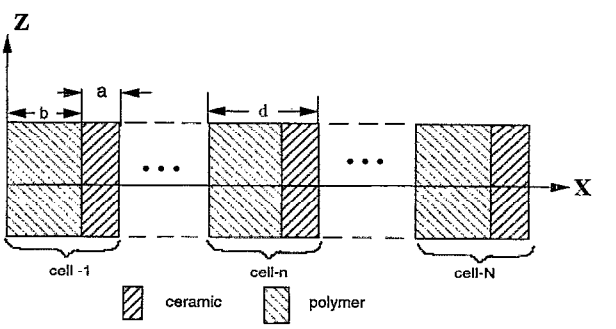

FIG. 1. Structure of a 2-2 ceramic-polymer composite, where a and b are the ceramic width and polymer width, respectively, $d=a+b$ is the pitch.

[a]Electronic mail: wcao@sun01.mrl.psu.edu

 0021-8979/95/78(7)/4640/7/$6.00

$$\psi_{np}=A_n e^{i(\omega t-k_p x)}+B_n e^{i(\omega t+k_p x)} \quad \text{(in polymer)}, \tag{1a}$$

$$\psi_{nc}=C_n e^{i(\omega t-k_c x)}+D_n e^{i(\omega t+k_c x)}+E e^{i\omega t} \quad \text{(in ceramic)}, \tag{1b}$$

where k_p and k_c are the wave numbers of the polymer and ceramic, respectively.

Basically, inside the polymer there is a forward wave and a backward wave with their amplitudes given by complex numbers (Appendix). While inside the ceramic, an additional position-independent vibration has to be included to specify the external drive. Among all the coefficients in Eqs. (1a) and (1b), E is a real number, A_n, B_n, C_n, and D_n are all complex numbers.

Similar to the case of single-wave propagation in composite, there are two boundary conditions at each interface, i.e., continuity and force equilibrium. Using Eqs. (1a) and (1b), these two conditions can be explicitly written at the nth P-C (from polymer to ceramic) interface, i.e., at $x = x_n^{PC}$,

$$A_n e^{-ik_p x_n^{PC}}+B_n e^{ik_p x_n^{PC}}=C_n e^{-ik_c x_n^{PC}}+D_n e^{ik_c x_n^{PC}}+E, \tag{2a}$$

$$Z_p(-A_n e^{-ik_p x_n^{PC}}+B_n e^{ik_n x_n^{PC}}) =Z_c(-C_n e^{-ik_c x_n^{PC}}+D_n e^{ik_c x_n^{PC}}), \tag{2b}$$

or

$$\begin{pmatrix} C_n \\ D_n \end{pmatrix}=\frac{1}{2Z_c}\begin{pmatrix} (Z_c+Z_p)e^{-i(k_p-k_c)x_n^{PC}} & (Z_c-Z_p)e^{i(k_p+k_c)x_n^{PC}} \\ (Z_c-Z_p)e^{-i(k_p+k_c)x_n^{PC}} & (Z_c+Z_p)e^{i(k_p-k_c)x_n^{PC}} \end{pmatrix}\begin{pmatrix} A_n \\ B_n \end{pmatrix}-\frac{E}{2}\begin{pmatrix} e^{ik_c x_n^{PC}} \\ e^{-ik_c x_n^{PC}} \end{pmatrix}$$
$$=[T(x_n^{PC})]\begin{pmatrix} A_n \\ B_n \end{pmatrix}-\frac{E}{2}\begin{pmatrix} e^{ik_c x_n^{PC}} \\ e^{-ik_c x_n^{PC}} \end{pmatrix}, \tag{3a}$$

where Z_p and Z_c are the acoustic impedance of the polymer and ceramic, respectively.

Similarly, we can obtain another relationship at $x = x_n^{CP}$, the nth C-P (from ceramic to polymer) interface,

$$\begin{pmatrix} A_{n+1} \\ B_{n+1} \end{pmatrix}=\frac{1}{2Z_p}\begin{pmatrix} (Z_p+Z_c)e^{i(k_p-k_c)x_n^{CP}} & (Z_p-Z_c)e^{i(k_p+k_c)x_n^{CP}} \\ (Z_p-Z_c)e^{-i(k_p+k_c)x_n^{CP}} & (Z_p+Z_c)e^{-i(k_p-k_c)x_n^{CP}} \end{pmatrix}\begin{pmatrix} C_n \\ D_n \end{pmatrix}+\frac{E}{2}\begin{pmatrix} e^{ik_p x_n^{CP}} \\ e^{-ik_p x_n^{CP}} \end{pmatrix}$$
$$=[T(x_n^{CP})]\begin{pmatrix} C_n \\ D_n \end{pmatrix}+\frac{E}{2}\begin{pmatrix} e^{ik_p x_n^{CP}} \\ e^{-ik_p x_n^{CP}} \end{pmatrix}. \tag{3b}$$

Therefore, the recurrence relation between the vibration amplitudes of the forward and backward waves in the nth and $(n+1)$th polymer elements is given by

$$\begin{pmatrix} A_{n+1} \\ B_{n+1} \end{pmatrix}=[T(x_n^{CP})][T(x_n^{PC})]\begin{pmatrix} A_n \\ B_n \end{pmatrix}-\frac{E}{2}[T(x_n^{CP})] \times\begin{pmatrix} e^{ik_c x_n^{PC}} \\ e^{-ik_c x_n^{PC}} \end{pmatrix}+\frac{E}{2}\begin{pmatrix} e^{ik_p x_n^{CP}} \\ e^{-ik_p x_n^{CP}} \end{pmatrix}. \tag{4}$$

It is interesting to see from Eq. (4) that the recurrence relation has similar features as the one for a single-source situation, in fact, the first term on the rhs of Eq. (4) is just the single-source transfer matrix. There are two additional terms proportional to the driving magnitude E, which will vanish upon the elimination of these internal vibration sources.

Once the vibration in the first cell is known, the amplitude in the nth cell can be calculated repeatedly using Eq. (4):

$$\begin{pmatrix} A_{n+1} \\ B_{n+1} \end{pmatrix}=\underbrace{[T(x_n^{CP})][T(x_n^{PC})][T(x_{n-1}^{CP})][T(x_{n-1}^{PC})]\ldots[T(x_1^{CP})][T(x_1^{PC})]}_{2n \text{ matrix}}\begin{pmatrix} A_1 \\ B_1 \end{pmatrix}$$
$$-\underbrace{[T(x_n^{CP})][T(x_n^{PC})][T(x_{n-1}^{CP})][T(x_{n-1}^{PC})]\ldots[T(x_1^{CP})]}_{(2n-1) \text{ matrix}}\begin{pmatrix} \frac{E}{2}e^{ik_c x_1^{PC}} \\ \frac{E}{2}e^{-ik_c x_1^{PC}} \end{pmatrix}$$

$$+[T(x_n^{CP})][T(x_n^{PC})][T(x_{n-1}^{CP})][T(x_{n-1}^{PC})]\ldots[T(x_2^{CP})][T(x_2^{PC})]\begin{pmatrix}\frac{E}{2}e^{ik_p x_2^{CP}}\\ \frac{E}{2}e^{-ik_p x_2^{CP}}\end{pmatrix}+\ldots$$

$$(2n-2)\ \text{matrix}$$

$$+(-)^{2n-m}[T(x_n^{CP})][T(x_n^{PC})][T(x_{n-1}^{CP})][T(x_{n-1}^{PC})]\ldots[T(x_{2n-m}^{CP})]\begin{pmatrix}V_1(x_{2n-m})\\ V_2(x_{2n-m})\end{pmatrix}$$

$$(2n-m)\ \text{matrix}$$

$$-[T(x_n^{CP})]\begin{pmatrix}\frac{E}{2}e^{ik_c x_n^{PC}}\\ \frac{E}{2}e^{-ik_c x_n^{PC}}\end{pmatrix}+\begin{pmatrix}\frac{E}{2}e^{ik_p x_n^{CP}}\\ \frac{E}{2}e^{-ik_p x_n^{CP}}\end{pmatrix}, \tag{5}$$

where

$$\begin{pmatrix}V_1(x_{2n-m})\\ V_2(x_{2n-m})\end{pmatrix}=\begin{cases}\begin{pmatrix}\frac{E}{2}e^{ik_c x_{2n-m}^{PC}}\\ \frac{E}{2}e^{-ik_c x_{2n-m}^{PC}}\end{pmatrix} & \text{if } 2n-m \text{ is odd}\\ \begin{pmatrix}\frac{E}{2}e^{ik_p x_{2n-m}^{CP}}\\ \frac{E}{2}e^{-ik_p x_{2n-m}^{CP}}\end{pmatrix} & \text{if } 2n-m \text{ is even.}\end{cases} \tag{6}$$

The vibration pattern for the ceramic elements can be calculated using Eq. (3a).

III. GLOBAL COORDINATES VERSUS LOCAL COORDINATES

Equation (5) could be simplified by using local coordinates if the structure is periodic. The idea is based on the fact that each wave function $\psi_{np}(x)$ is valid only in a spatial interval of $(n-1)d<x<nd-a$, where a is the width of ceramic and $d=a+b$ is the period with b being the width of the polymer.

Let us introduce a local coordinate

$$y=x-(n-1)d \tag{7a}$$

for the forwarding wave and

$$y'=x-(nd-a) \tag{7b}$$

for the backward wave so that each wave function is considered to be generated at the nearest interface of the position of interest x, then the transfer matrix Eq. (5) can be greatly simplified.

Using these local coordinates, we can rewrite the wave functions Eqs. (1a) and (1b) in the following form:

$$\psi_{np}=\hat{A}_n e^{i\{\omega t-k_p[x-(n-1)]d\}}+\hat{B}_n e^{i\{\omega t+k_p[x-(nd-a)]\}}\quad\text{(in polymer)}, \tag{8a}$$

$$\psi_{nc}=\hat{C}_n e^{i\{\omega t-k_c[x-(nd-a)]\}}+\hat{D}_n e^{i[\omega t+k_c(x-nd)]}+Ee^{i\omega t}\quad\text{(in ceramic)}, \tag{8b}$$

where

$$\hat{A}_n=A_n e^{-ik_p(n-1)d}, \tag{9a}$$

$$\hat{B}_n=B_n e^{ik_p(nd-a)}, \tag{9b}$$

$$\hat{C}_n=C_n e^{-ik_c(nd-a)}, \tag{9c}$$

$$\hat{D}_n=D_n e^{ik_c nd}, \tag{9d}$$

compared with Eqs. (1a) and (1b).

The physical meaning of Eqs. (8a) and (8b) is very clear. Each polymer-ceramic interface now becomes the origin of the acoustic source whose strength is the superposition of all the waves propagating inside the structure. Again, we must note that the coefficients are all complex numbers except E. It can be shown that the recurrence relation becomes much simpler using the local coordinate representation:

$$\begin{pmatrix}A_{n+1}\\ B_{n+1}\end{pmatrix}=[T]\begin{pmatrix}A_n\\ B_n\end{pmatrix}+[V], \tag{10}$$

where

$$[T]=\frac{1}{4Z_cZ_p}\begin{pmatrix} e^{-k_pb}[4Z_cZ_p\cos(k_ca)-2i(Z_c^2+Z_p^2)\sin(k_ca)] & -2i(Z_c^2-Z_p^2)\sin(k_ca) \\ 2i(Z_c^2-Z_p^2)\sin(k_ca) & e^{ik_pb}[2i(Z_c^2+Z_p^2)\sin(k_ca)+4Z_cZ_p\cos(k_ca)] \end{pmatrix}, \tag{11}$$

$$[V]=\frac{E}{2}\begin{pmatrix} 1-\cos(k_ca)+i\frac{Z_c}{Z_p}\sin(k_ca) \\ e^{ik_pb}\left[1-\cos(k_ca)-i\frac{Z_c}{Z_p}\sin(k_ca)\right] \end{pmatrix}. \tag{12}$$

Note that both $[T]$ and $[V]$ are independent of n. One now only needs to perform the T-matrix calculation once. The vibration in the nth cell can be easily derived if vibration in the first cell is known. For instance, the polymer vibration recurrence relation now becomes

$$\begin{pmatrix} A_{n+1} \\ B_{n+1} \end{pmatrix}=[T]^n\begin{pmatrix} A_1 \\ B_1 \end{pmatrix}+[[T]^{n-1}+[T]^{n-2}+\cdots+[T]+[I]][V]=[T]^n\begin{pmatrix} A_1 \\ B_1 \end{pmatrix}+[[I]-[T]^n][[I]-[T]]^{-1}[V], \tag{13}$$

where $[I]$ is the unit matrix and the exponent -1 represents the matrix inversion. The above recurrence relation can be further simplified to become

$$\begin{pmatrix} A_{n+1}-V_1' \\ B_{n+1}-V_2' \end{pmatrix}=[T]^n\begin{pmatrix} A_1-V_1' \\ B_1-V_2' \end{pmatrix} \tag{14}$$

with

$$\begin{pmatrix} V_1' \\ V_2' \end{pmatrix}=[[I]-[T]]^{-1}\begin{pmatrix} V_1 \\ V_2 \end{pmatrix}. \tag{15}$$

Equation (14) is much simpler for numerical calculations compared to Eq. (5) which involves explicitly the coordinates of all the cells.

IV. DAMPING EFFECTS

In a ceramic-polymer composite transducer, high damping in the polymer is desirable for reducing the ringing down to increase the resolution and the bandwidth of the transducer. We can study this situation by introducing complex wave numbers and acoustic impedance when the multisource T-matrix technique described in Secs. II and III is used.

Let α_p and α_c represent the damping constants of the polymer and ceramic, respectively, the damped waves may be written in the following form:

$$\psi_{np}=A_ne^{-\alpha_px}e^{i(\omega t-k_px)}+B_ne^{\alpha_px}e^{i(\omega t+k_px)} \quad \text{(in polymer)}, \tag{16}$$

$$\psi_{nc}=C_ne^{-\alpha_cx}e^{i(\omega t-k_cx)}+D_ne^{\alpha_cx}e^{i(\omega t+k_cx)}+Ee^{i\omega t} \quad \text{(in ceramic)}. \tag{17}$$

If we introduce two complex wave numbers

$$\tilde{k}_p=k_p-i\alpha_p, \tag{18}$$

$$\tilde{k}_c=k_c-i\alpha_c, \tag{19}$$

Eqs. (15) and (16) will have the same format as that of Eqs. (1a) and (1b). In addition, we can generalize the definition of the acoustic impedance to include an imaginary part,

$$\tilde{Z}_p=\frac{\tilde{k}_p\nu^p}{\omega}=Z_p-i\frac{\alpha_p\nu^p}{\omega}, \tag{20}$$

$$\tilde{Z}_c=\frac{\tilde{k}_c\nu^c}{\omega}=Z_c-i\frac{\alpha_c\nu^c}{\omega}. \tag{21}$$

All the derivations in Secs. II and III can be duplicated for the damped system with these complex wave numbers, $\tilde{k}_p$ and $\tilde{k}_c$, and the complex impedance, $\tilde{Z}_p$ and $\tilde{Z}_c$. The results are the same except replacing the real, k_p, k_c, Z_p, and Z_c by their complex counterpart. The resonance magnitude will be greatly reduced as we will see from the calculations below.

V. RESULTS AND DISCUSSIONS

In a composite transducer, the polymer phase can be chosen to be lossy in order to reduce the level of spurious resonance from the shear waves, while the damping in ceramic is relatively small and have little flexibility for adjustment. For simplicity damping is introduced only in the polymer ($\alpha_c=0$) in the calculations. The damping factor in our calculation is assumed to be a linear function of frequency

$$\alpha_p=\alpha_0(5.41\times10^{-5}f-20.49)/m, \tag{22}$$

where f is the frequency in Hertz and α_0 is an adjustable factor. The coefficients were so chosen that when $\alpha_0=5$, the rhs of Eq. (22) divided by the conversion factor ln 10=2.3 will give the α_p value in dB.

Most of the composite transducers operate in the thickness mode, i.e., resonance in the z direction shown in Fig. 1. Because the pitch scale (the period) d is usually made very small in conventional transducer design in order to make the pitch resonance will be at a much higher frequency than the thickness mode. The transducer will not function well when the spurious transverse modes occur.

In order to study the relevant shear modes in a multisource system, we define an average amplitude of the ceramic components M as a measure to characterize those relevant shear modes,

$$M=\frac{1}{N}\sum_{n=1}^{N}\int_{\text{ceramic}}|\psi_c|dx, \tag{23}$$

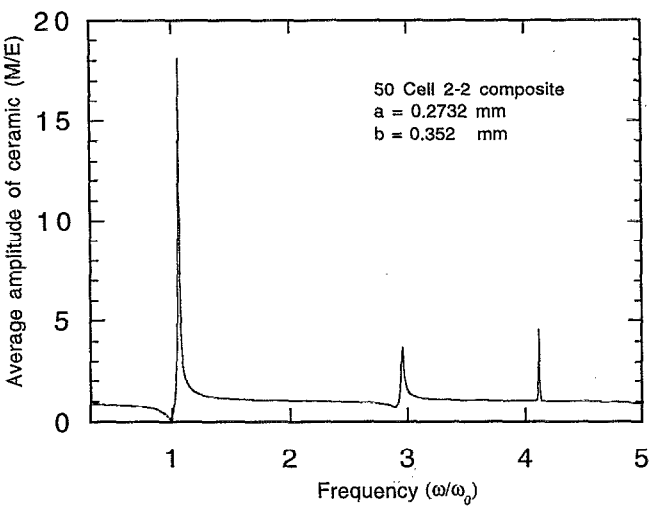

FIG. 2. Frequency dependence of the average ceramic vibration amplitude for shear wave propagation in a multisource driven system. Polymer damping is chosen at $\alpha_0=2$.

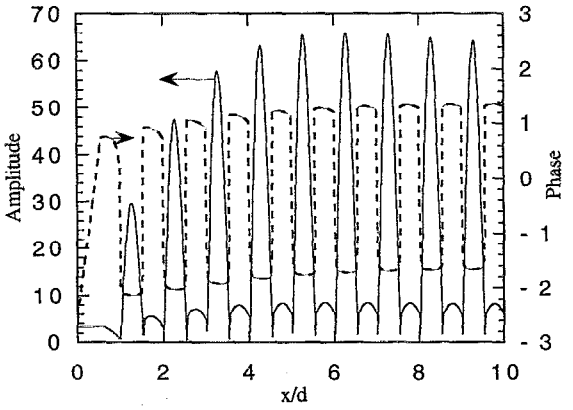

FIG. 3. Space profile of the vibration amplitude and phase for a 50 cell composite at the main peak frequency of $\omega=1.056\omega_0$.

where the integration is on the ceramic element only to account for the piezoelectric effect. N is the total number of the cells in the composite.

To be more general, M is normalized by the magnitude of the applied drive $|E|$, and the frequency is normalized by the half wavelength shear wave resonance frequency of the polymer element,

$$\omega_0=\frac{\pi v_p}{b}, \tag{24}$$

where v_p is the shear acoustic velocity of the polymer.

Figure 2 shows the frequency dependence of M for a 50 cell 2-2 composite with the polymer width $b=0.352$ mm and the ceramic width $a=0.2732$ mm (44% ceramic by volume). The physical properties of ceramic and polymer used for the calculations are given in Table I. Figure 2 shows three peaks of M, corresponding to the pitch resonance, its third harmonic, and a higher shear resonance. Other peaks at much lower frequencies related to the overall size of the composite structure have much smaller magnitude and therefore ignored here.

The most pronounced low-frequency peak is the one near ω_0, or $\omega/\omega_0\sim1$, corresponding to the pitch resonance, we call it the main peak. In transducer design, this main peak is the most interesting one which determines the frequency limit for the composite transducer. In what follows we will devote most of the effort to study this main peak.

In order to see the physical meaning of those peaks in Fig. 2, we have calculated the space profile and phase variation inside the composite at these corresponding peak frequencies. Figure 3 is the space profile of a 50-cell composite at the main peak frequency of $1.056\omega_0$. We can see clearly that the pattern corresponds to the full wavelength pitch resonance with the ceramic and polymer elements vibrating 180° out of phase. It is important to note that this is the first excited mode in this structure due to the symmetry of the driving force applied to the composite, whereas in the single drive analysis, other nonpiezoelectric active modes will also appear.[10] The second important point that should be noted in Fig. 3 is the strong edge effects, which are unavoidable in a finite system. The edge effects can be seen more clearly in Fig. 4 which displays the space profile and the phase variation of several composites made of 6, 10, and 50 cells. Both the magnitude and the phase are affected by the composite size. As a consequence, the main peak of the average magnitude also shows some degree of size dependence, both the magnitude and the peak frequency are smaller for composites with lesser cells, but these values saturate after $N>100$.[11]

The amplitude of the main peak is affected strongly by the damping in the polymer phase as shown in Fig. 5. The peak value $M_{\max}$ changes drastically with the increase of the damping coefficient α_0 defined in Eq. (22). This suggests that lossy polymer can play an important role in reducing the effects of the pitch resonance.

TABLE I. Material properties for the ceramic and polymer constituents of the 2-2 composite.

Ceramic:	$c^c_{55}=2.4$ (10^{10} N/m^2),	$\rho_c=7800$.
Polymer:	$c^p_{55}=1.59$ (10^9 N/m^2),	$\rho_c=1160$.

VI. EFFECTS OF RANDOMIZATION

Considering the fact that the main peak is from the pitch resonance due to the periodic nature, it should be reduced or eliminated if the periodicity is destroyed.[12–15] There are two kinds of fabrication processes in making a composite, one is placing ceramic elements of the same size with certain spacing in between and then filling in the gaps with polymer resin; the other is to dice a solid ceramic to create the kerfs and then filling in those kerfs with polymer. The former has a fixed ceramic dimension, or constant a, while the latter has a constant polymer width b (saw blade thickness). Therefore, randomizing a would be easier for the latter fabrication process and randomizing b would be easier for the former fabrication process. Using the multisource T-matrix techniques

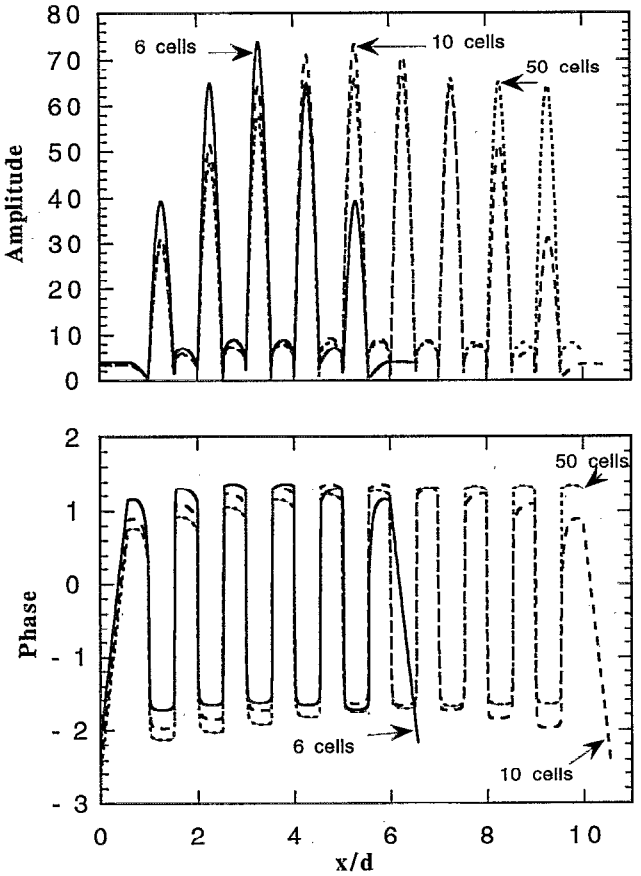

FIG. 4. Comparison of the vibration amplitude and phase for composites consisting 6, 10, and 50 cells. Only the first 10 cells were plotted for the 50 cell composite.

described in Sec. II, we have studied the effects of randomization for the multisource driven system in both cases of a random and b random.

Figure 6 shows the effects of randomizing ceramic spacing b. It is expected that the randomization of b will have a strong effect because the main resonance peak shown in Fig. 2 appears to be close to the polymer half-wavelength resonance frequency.

The randomized ceramic spacing b_i is chosen according to the following formula:

$$b_i=(1-\chi)b_0+\chi C_r r_i, \quad C_r=\frac{Nb_0}{\Sigma_i^N r_i}, \tag{25}$$

where b_0 is the arithmetic mean of the ceramic spacing (or polymer width), N is the total number of cells, r_i ($i=1,\ldots,N$) is a set of random numbers between 0 and 1, and χ is the percentage of randomization which is defined to be the variable percentage of b_i. We have studied the cases of χ=5%, 10%, 20%, and 50%.

As shown in Fig. 6, the resonance nature changes dramatically with the introduction of randomness. The magnitude of the main resonance peak is reduced by 40% with only *5% randomness*. At the same time, there are more small bumps created in the vicinity of the original main peak. Theoretically speaking, more randomness in the structure is

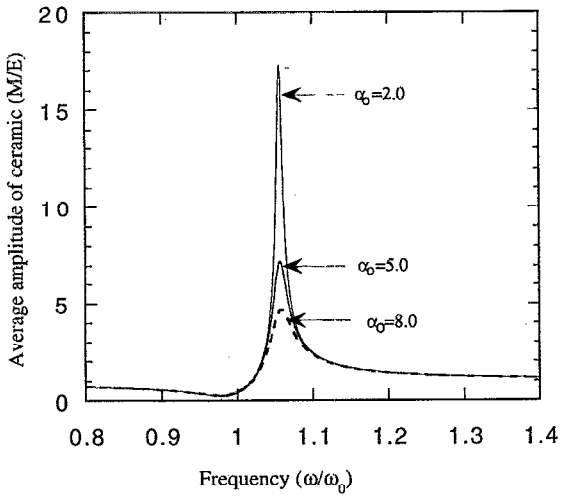

FIG. 5. Effect of damping on the main resonance peak. α_0 are chosen to be 2, 5, and 8, respectively.

better in terms of dispersing the main resonance peak, but the effect is the strongest within the first 20% randomness.

We also found that the influence of randomizing b on the main peak becomes much weaker for high ceramic volume percent composites for which the major contribution to the main low-frequency resonance will come from the ceramic. On the other hand, randomizing a has different effects as shown in Fig. 7, where the results were calculated for a composite with 45% ceramic. When the ceramic percentage is less than 60% ceramic volume content, the main low-frequency peak is reduced but still relatively strong even for 50% randomness of a. Interestingly, the shape of the peak remains practically the same. However, when the ceramic percent is more than 70%, the shape of the main peak will be destroyed through randomizing a. Figure 8 shows the calcu-

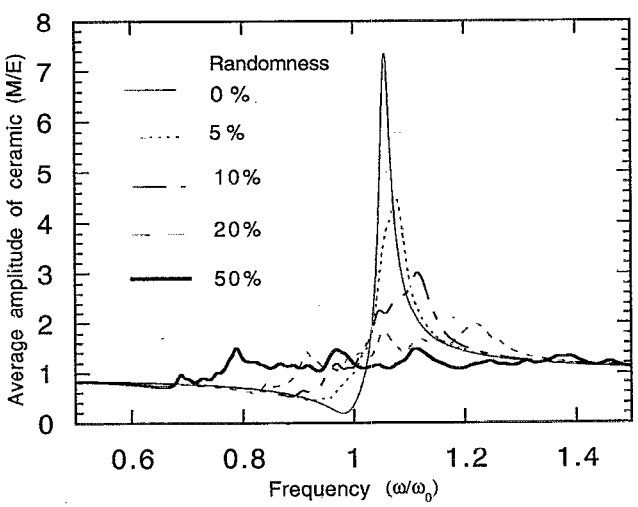

FIG. 6. Effects of randomizing b for a composite with 45% ceramic volume content. The percentages of randomness are 5%, 10%, 20%, and 50%, respectively. The effectiveness decreases with the increase of ceramic content.

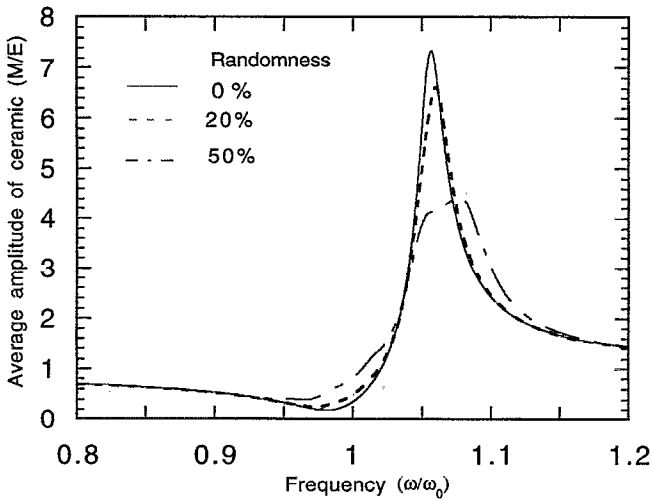

FIG. 7. Effects of randomizing a for a 45% ceramic composite. The percentages of randomness are 5%, 10%, 20%, and 50%, respectively. The influence on the low-frequency main peak is much smaller compared with randomizing b as shown in Fig. 6.

lated results for a composite contains 80% ceramic. We can see that the effect of randomizing a is much larger compared with the results shown in Fig. 7.

VII. SUMMARY AND CONCLUSIONS

We have derived the recurrence relation for the vibration amplitude among different cells in a multisource driven stratified structure using an extended multisource T-matrix technique. Ceramic-polymer composites with 2-2 connectivity is a perfect example of such situation. The new criteria Eq. (23) introduced here can directly identify the relevant shear modes that affect the thickness mode operation. Analyses show that the lowest shear mode, corresponding to the pitch resonance, is the most important mode which couples strongly to the thickness resonance in a periodic composite transducer.

The pitch resonance can be destroyed by randomization. For moderate ceramic volume content (60% or less), the main peak is primarily linked to the spacing between the ceramics. In this case, we found that randomizing the spacing between ceramics, i.e., b is much more effective than randomizing a, the ceramic width. On the other hand, for very high percentage ceramic content (70% or more), the effect of randomizing a becomes more effective than randomizing b since the main low-frequency peak is tied more to the ceramic dimension. These results can provide useful guidelines for making random composite transducers.

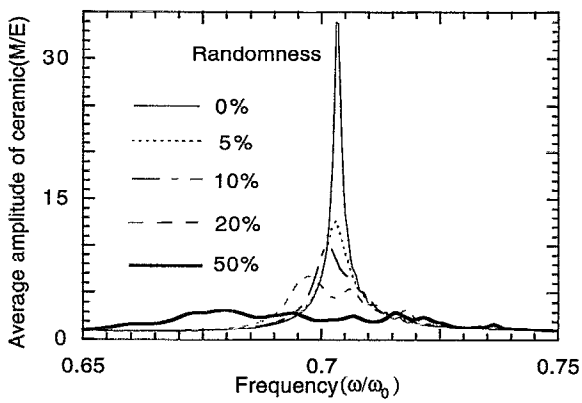

FIG. 8. Effects of randomizing a for a composite with 80% ceramic volume content. The percentages of randomness are 5%, 10%, 20%, and 50%, respectively. Note this peak does not appear for a low ceramic content composite, for which the lowest peak is near ω_0 as shown in Fig. 6.

ACKNOWLEDGMENT

This research is supported by the Office of Naval Research under Grant No. N00014-92-J-1501.

APPENDIX

Assuming there are m acoustic sources located at $-a_1,-a_2,\ldots,-a_m$ sending waves to forward direction, then the wave form at position x is the linear superposition of these waves:

$$\psi(x)=A_1e^{i[\omega t-k(x+a_1)]}+A_2e^{i[\omega t-k(x+a_2)]}+\cdots +A_me^{i[\omega t-k(x+a_m)]}=[A_1e^{-ika_1}+A_2e^{-ika_2}+\cdots +A_me^{-ika_m}]e^{i(\omega t-kx)}=Ae^{i(\omega t-kx)}, \quad \text{(A1)}$$

where

$$A=A_1e^{-ika_1}+A_2e^{-ika_2}+\cdots+A_me^{-ika_m}$$

is a complex number. Therefore, both the forward and backward waves can be written as a simple wave form even for the multisource system except the amplitude is now a complex number.

For the ceramic elements the wave function also should include the uniform driving of the external field.

[1] W. T. Thomson, J. Appl. Phys. **21**, 89 (1949).
[2] E. H. Lee and W. H. Yang, SIAM J. Appl. Math. **25**, 492 (1973).
[3] C. G. Oakley, Ph.D. thesis, The Pennsylvania State University, 1991.
[4] Y. Wang, E. Schmidt, and B. A. Auld, Proceedings of IEEE 1986 Ultrasonic Symposium, 1986, p. 685.
[5] B. A. Auld, H. A. Kunkel, Y. A. Shui, and Y. Wang, Proceedings of IEEE 1983 Ultrasonic Symposium, 1983, p. 554.
[6] C. Potel and J. F. Belleval, J. Acoust. Am. Soc. **93**, 2669 (1993).
[7] Y. Wang and B. A. Auld, Proceedings of IEEE 1985 Ultrasonic Symposium, 1985, p. 637.
[8] Y. Wang, Ph.D. thesis, Stanford University, 1986.
[9] A. M. B. Braga and G. Hermann, J. Acoust. Soc. Am. **91**, 1211 (1991).
[10] W. Cao and W. Qi, J. Appl. Phys. **78**, 4627 (1995).
[11] W. Cao and W. Qi (unpublished).
[12] J. A. Hossack, B. A. Auld, and H. D. Batha, Proc. IEEE 1991 Ultrasonic Symposium, 1991, p. 651.
[13] B. A. Auld and J. A. Hossack, Electron. Lett. **27**, 1284 (1991).
[14] P. Sheng and Z. Zhang, Phys. Rev. Lett. **57**, 1879 (1986).
[15] T. R. Kirkpatrick, Phys. Rev. B **31**, 5746 (1985).